Industrial Engineering Journal
ISSN: 0970-2555
Volume : 50, Issue 9, No. 1, September : 2021

Multi-Scale Modeling of Fracture Behavior in Fiber-Reinforced Polymer Composites

[1]R Sai Syam, [2]Dr. M Ashok Kumar, [3]G H Manjunath

[1, 3] Assistant Professor, Department of Mechanical Engineering, Narsimha Reddy Engineering College, Secunderabad, Telangana
[2]Professor, Department of Mechanical Engineering, Narsimha Reddy Engineering College, Secunderabad, Telangana

Abstract:

Fiber reinforced polymer matrix composites (FRPMCs) often experience intra laminar fiber-matrix fracture, sometimes referred to as splitting, during tensile failure. Numerical modeling issues are related to the prediction of this failure mode and its impact on a macroscopically homogenized model. A very effective two-scale model is shown, which utilizes the analytical technique of the micromechanics 2-concentric cylinder (2CYL) for pre-peak nonlinearity and interfaces with the 3D orthotropic smeared crack approach (SCA) for post-peak softening behavior. Using typical 3D finite elements, a homogenized ply is represented in a way that allows for the explicit capture of a matrix fracture with regard to the ply angle orientation. By forecasting the grip-to-grip longitudinal split in a 00 ply, mixed-mode matrix cracking in 450 ply, transverse matrix cracking in 900 ply, and the failure of laminate comprising these plies, the suggested method's capacity is shown. It is discovered that the predictions made by the suggested approach and the related experimental results accord rather well.

1. Introduction

A significant number of researchers have conducted experiments and noticed the phenomenon of intralaminarfiber-matrix splitting failure [6–9]. In the case of laminated composites, this mechanism of failure is significant, and the use of a validated computational tool is an absolute must when designing with FRPMCs. The enormous number of matrix fractures that were seen in studies [10–15] is still a hard situation that cannot be replicated by simulation, despite the significant efforts that have been made toward modeling progressive failure. Each individual ply is made up of hundreds of fibers that are encased in a matrix material and packed in a variety of different configurations. As a result of the combined local stress condition, the matrix that is contained inside the ply and in between the fibers develops micro-fractures; nevertheless, these cracks do not expand fast since the fibers are preventing their growth. From the perspective of the lamina, these matrix micro-cracks are responsible for the pre-peak nonlinear behavior of the lamina. Over time, they will eventually grow into a single macro-crack, which will ultimately result in the failure of a two-piece ply in isolation.

When studying a bigger structure, it is computationally costly to model individual fibers. However, it is possible to model the fibers and matrix individually at a microscopic representative volume element (RVE) level [16–22]. Additionally, numerical simulations may be carried out in order to capture this failure behavior. However, as demonstrated in this article, a two-scale model of a homogenized lamina is capable of accurately capturing the fiber-matrix failure mode. Furthermore, when this foundational modeling approach for a

lamina is utilized in a three-dimensional model of a laminate, it is also observed to accurately predict laminate failure. As a result, the modeling approach that is presented here can be utilized for predictive modeling. The author who corresponds. electronic mail address: awaas@umich.edu (A.M. Waas), which will result in a considerable decrease in the number of tests that are required, which will in turn lead to a significant cost savings.

Fiber-reinforced polymers are becoming more essential materials for structural applications across a wide range of industries. In the field of civil engineering, for instance, there are a number of noteworthy uses of unidirectional (UD) carbon fiber reinforced polymers (CFRP) [1,2,3,4]. There are a number of mathematical regimes that have been developed in order to estimate the strength of these materials [9]. These regimes include analytical [5,6], semi-analytical [7], and numerical models [8]. As a result of the fact that homogenized macroscale models [10] are unable to accurately reflect the failure processes of a composite material, micromechanical models have been created as an alternative [11]. Phenomenological models, such as shear lag and fiber bundle models [12], and numerical models that make use of the finite element method (FEM) [9] are two categories that may be taken into consideration when discussing micromechanical models. Although both kinds of micromechanical models take into consideration the interactions between fiber and matrix, only numerical models have the capacity to completely represent the complex nature of damage progression in composites [13]. This is because numerical methods describe the interactions between the matrix and the fiber. They are able to provide a realistic description of the process by which failure develops, as well as the manner in which flaws that are relatively minor in comparison to the microstructural characteristics influence the performance of a composite. When it comes to creating laminates, numerical micromodels may also be used to address ply properties without the need for experimental investigations. A number of analytical models have been devised for the purpose of solving the homogenized properties based on the characteristics of the component entities [14]. On the other hand, the analytical models may not always operate in a reliable manner, particularly in situations when the fiber volume percentages are more than 0.6 [15]. The analytical answers, on the other hand, are quite easy to implement. For the purpose of computing mechanical finite element models, these homogenized macroscopic material characteristics are required as an input. Micromechanical modeling is important not only during the manufacture of a component but also throughout its service life. It is possible that it might give a way to mimic the reaction of a structure as a consequence of various sizes and kinds of damage that occur during service, and as a result, it could be incorporated into relevant condition monitoring systems. In addition to this, it enables continuous review and offers improved information on the measures that must be taken in the event that damage is discovered and defined via the use of non-destructive evaluation [16]. To put it another way, it improves the capability of determining the residual strength and determining whether or not a component may continue to be used in service. However, in order to provide findings that can be relied upon, micromechanical models need to have the appropriate input, which includes the characteristics of the fibers and matrix (also known as component qualities) as well as the microstructure.

Anisotropic composite materials provide a number of challenges, including the difficulty of obtaining component attributes and confirming the homogenized product. However, materials that are transversely isotropic, such as carbon fiber and unidirectional fiber-reinforced composites, only have five material constants that are independent of one another [17]. From the results of instrumented tensile testing, it is not difficult to determine the longitudinal Young's modulus of the fiber [18,19]. In addition, the rule of mixing has been thoroughly established for the axial characteristics of UD composites, which enables the application of inverse micromechanics with complete assurance. Direct measurements of the transverse Young's modulus E2f have been carried out via the use of nanoindentation [14], and the findings have been discovered to be marginally greater than those produced through the use of a variety of analytical inverse micromechanics solutions [20]. Quantification of the transverse Young's modulus of carbon fibers has also been accomplished by the use of resonance frequencies [21]. It is difficult to get the remaining three elastic constants of a single filament using experimental means. A significant number of publications rely on the use of inverse micromechanics and the measurement of composite characteristics [22]. Others mention sources that are difficult to access [25], while others just assume certain elastic qualities [22,23,24]. Some modeling works simply assume certain elastic properties.

To the greatest extent feasible, the microstructure that has been simulated ought to provide an accurate description of parameters including the fiber volume percentage, packing, size, and shape. In contrast to random packing generators, which produce a more realistic distribution of fibers [26], periodic square or hexagonal fiber packing is an idealized situation. However, large fiber volume fractions provide a challenge for the generators [27]. It has been shown that the transverse elastic constants are affected by the difference between periodic and random packing [15]. When it comes to strength models, fibers that are very near to one another might result in a considerable increase in stress concentration factors [26]. However, the stress recovery distance is reduced since the matrix is often more rigid in the immediate area. As a result, the kind of packing does not have a significant impact on the uniaxial loading of UD CFRPs in the fiber direction [28]. Debonding and matrix plasticity, on the other hand, have the potential to alter the findings [29], and off-axis loading need random packing in order to get correct results [30].

The purpose of this study is to explain the process of developing a multiscale microstructure-based model and to validate that model via experimentation. At the end of the day, the purpose of this effort is to develop a macroscale strength model that takes into account microstructural faults without the requirement for experimental model update or calibration. The following is the outline of the contents of the paper: To begin, a description is given of the overall framework of the multiscale method as well as the prerequisites for a micromechanical model. The next step is to describe the numerical techniques that may be used to calculate the characteristics of composites by making use of the information that was established in the previous stage. Lastly, the composite characteristics are used in order to acquire pertinent boundary conditions (BCs) for the purpose of loading the initial micromodel and modeling the impact that a defect has on the strength of the material. A comparison is made between the findings of the modeling and the measurements of a pultruded UD CFRP beam at each incremental stage.

2. Methods and Materials

A common multiscale method [31] is followed by the workflow, which is shown in Figure 1. In this technique, microscopic behavior is characterized by means of a representative volume element (RVE), and the first stage involves homogenization of the RVE in order to mimic the global reaction via simulation. By adjusting the size of the RVE until the homogenization of characteristics is achieved, a statistical volume element (SVE) is created. This allows for the evaluation of the statistical representation of the microstructure. Although not all of the individual input parameters are required fully known, the sensitivity of the homogenized qualities to changes in component properties, such as fiber and matrix properties, is analyzed with the purpose of determining the significance of each individual parameter. The purpose here is to avoid using experimental calibration [33] or inverse micromechanics, even if it is possible to measure homogenized qualities by experimentation [32]. This may be attributed to two different factors: To begin, every time an input parameter is altered, it is necessary to do experimental work, which may be both time-consuming and costly. Using inverse micromechanics or model calibration eliminates the need for experimental validation, which brings us to our second statement. A macroscopic model that takes into account the component geometry, boundary conditions, and load scenarios is the second phase in the process. This step involves inserting the homogenized characteristics into the model. By loading the component and comparing the observed strain values with the simulated strain, it is possible to provide experimental validation of the response of the macroscopic model. Identification of key locations within the structure is accomplished by the usage of the macroscopic model. In order to ensure that the displacements and boundary conditions for the RVE are applicable to the real application, the third stage in the workflow entails making use of the crucial locations for defining the RVE. Now, it is possible to analyze at microscale under stress conditions that are relevant to real-life applications the influence of known faults that were discovered using advanced non-destructive testing [16] or hypothetical defects. There is thus the possibility of calculating the simulated failure strength of a damaged component and comparing it to the failure loads that were acquired via experimentation. To get the best possible outcome, this procedure should enable the assessment of the residual strength of a damaged component based on the findings of an in-service inspection.

Industrial Engineering Journal
ISSN: 0970-2555
Volume : 50, Issue 9, No. 1, September : 2021

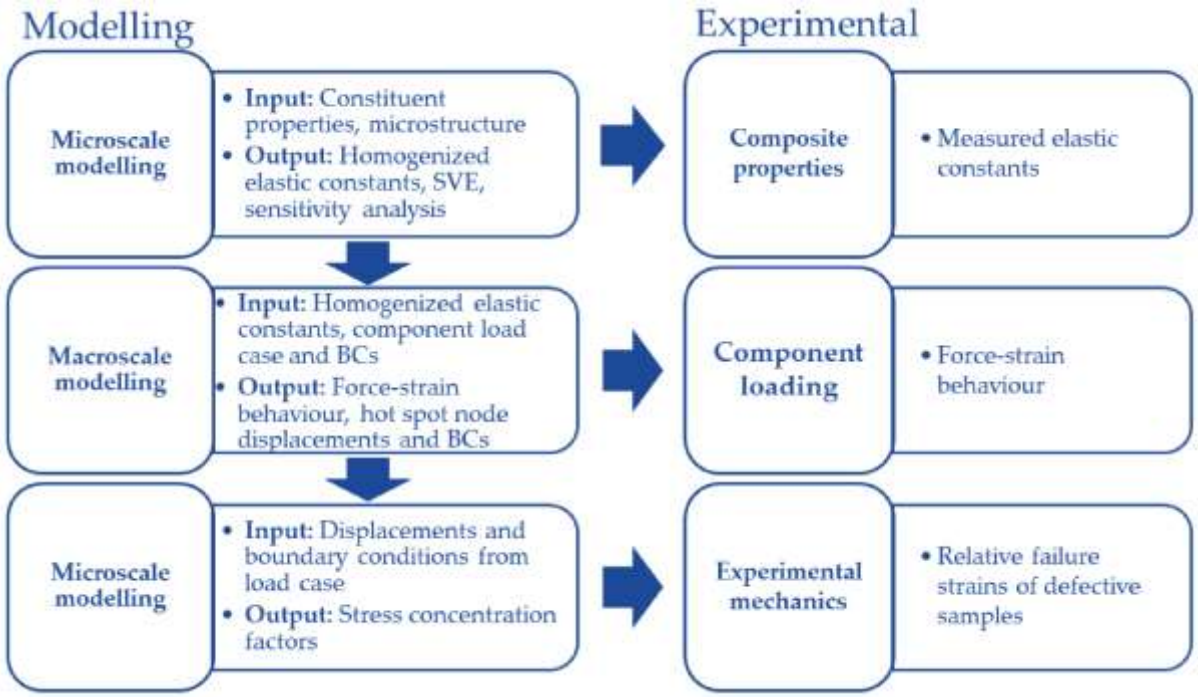

3. Proposed Mechanism

The three-point bending of a pultruded UD CFRP beam is the subject of the macroscopic model and case study research that is given in this article. Obtaining homogenized composite characteristics and creating the RVE are both accomplished via the use of constituent properties and micrographs. The results of the macroscopic simulation are utilized to determine the crucial position, and the node displacements at that site are used as a load case for the RVE in order to analyze the impact that porosity has on the strength of the beam. Validation via experimentation is carried out at each phase.

3.1. Constituent Properties

An industrial manufacturing factory used a heated pultrusion die in order to make the carbon fiber reinforced plastic (CFRP) rods. Standard modulus (high strength) polyacrylonitrile-based (PAN) carbon fiber reinforcement and epoxy resin matrix are the components that make up the composite. The constituent characteristics that were provided by the CFRP manufacturer were used in this work, which is a source that is often utilized in modeling publications [34,35]. A total of two Young's moduli, E1 and E2, as well as one shear modulus, G12, and two Poisson's ratios, v12 and v23, are used in this research. The following are the material constants that are most likely to be obtained by experimental means. "1" is used to indicate the direction of the fibers, while "2-3" is used to indicate the transverse plane.

The experimental verification of the qualities of the constituents that were provided was carried out utilizing instrumented nanoindentation whenever it was practicable to do so. Indentation was carried out on longitudinal and transverse cross-sections of the UD CFRP material with the purpose of validating E1f, E2f, and Em. The subscripts "f" and "m" stand for fiber and matrix, respectively. The indentation was carried out using a CSM Instruments

MCT tester (Needham, Massachusetts, United States of America). along order to get ten measurements, specimen cross-sections were wet sanded to a grit of FEPA P4000. These measurements were taken along a line with intervals of 10 µm. Due to the fact that the indentation modulus stabilizes at relatively high values [14,36,37], a depth of 0.1 µm was chosen for the indentation. On the other hand, deeper indentation was avoided in order to reduce the risk of fracture and maintain the continuity of the area function of the sphero-conical tip. After analyzing the data, it was clear which indentations had made contact with the fiber and which were located on the matrix. It was determined that the direction of the measurement line for the transverse sample was perpendicular to the direction of the fiber, which indicates that no two measurements were taken from the same filament. The settings for the indentation process are as follows: the indenter is a sphero-conical SB-B28, the tip radius is 2 µm, the cone full angle is 90°, the indentation depth is 0.1 µm, the loading rate is 0.8 mN/min, the dwell period is 30 seconds, and the data collection rate is 10 Hz.

Using the force-displacement data, the first unloading slope was calculated and established. Due to the fact that the power-law fit that is generally used and that was presented by Oliver and Pharr [38] did not generate high-correlation fits, a quadratic polynomial was taken into consideration. It was necessary to remove any permanent displacement (hf) from the data, and then it was necessary to impose intersection with the origin. For the purpose of determining the initial unloading slope, also known as contact stiffness, S [39], the derivative of the polynomial fit at maximum displacement was used. For the purpose of calculating the contact depth (hc), the contact stiffness was used, and the value ε was set to 0.75, as suggested in reference [38]. Calculating the projected contact area and, thus, the indentation modulus M according to Vlassak's definition [40] required the use of the contact depth while doing so. When it is known what the parameters of the indenter are, it is simple to compute the indentation modulus of the isotropic matrix by utilizing the Oliver and Pharr technique [38]. In the case of an anisotropic material, where the contact area is circular, a different solution is used [41,42]. In this case, the concept is to solve all five stiffness constants by using a five-equation system. This is accomplished by including three previously known stiffness constants and two perpendicular indentation results via the system. The findings of a one-at-a-time sensitivity analysis revealed that none of the engineering constants that were added had a substantial impact on the outcomes on their own. For the purpose of the sensitivity analysis, each engineering constant was gradually increased or decreased by a factor of two or one-half. The values that were obtained for E2f were kept within a deviation of ten percent from the reference scenario. It was the indentation modulus that had the most significant impact, and its relationship was very close to being linear.

3.2. Microstructure

Because a strength model is the end aim in this situation, the morphology of the model is generated by using the actual microstructure of a pultruded carbon fiber reinforced plastic beam. In order to examine the pultruded carbon fiber reinforced plastic material, high-resolution X-ray microtomography was performed [16]. However, it was discovered that the microtomography voxel data could not be used to differentiate between fiber and matrix, and as a result, a 2.5D technique was chosen. There is an assumption that the fibers are completely straight, despite the fact that the CT data [16] and transverse cross-sections [3]

show that there is some fiber waviness. A Hitachi SU1510 variable pressure scanning electron microscope (VP-SEM) from Tokyo, Japan was used for imaging of two-dimensional cross-sections, and backscatter electron (BSE) detection was utilized for the imaging process. To get a larger yield of back-scattered electrons in comparison to lesser acceleration voltages, the incoming electrons were accelerated with a potential of 25 kV. This was done in order to achieve the desired result. Additionally, a binary color map and manually modified threshold criteria are used in order to conduct an analysis of the fiber volume fraction derived from that picture. By introducing water to the resin bath at the pultrusion line, defects were introduced into the material that was the result of the pultrusion process. Because of the different densities of water and resin, heterogeneous dispersion, and the continuous nature of the pultrusion process, it is impossible to regulate the pore content that is produced as a consequence. As a consequence of this, optical microscopy was required in order to quantify the typically occurring pore size and the pore content that was produced. The photographs were captured with a Nikon DigitalSight DS-U1 camera, which had a resolution of 1600 × 1200 pixels. The microscope utilized was a Nikon Epiphot 200, which was manufactured in Tokyo, Japan. When it comes to the microstructure that contains pores, the 2.5D method of producing a 3D mesh does not permit the use of direct image-based meshing. An section of the microstructure that is abundant in resin is used instead in order to symbolize the impact of porosity.

The experimental verification of the qualities of the constituents that were provided was carried out utilizing instrumented nanoindentation whenever it was practicable to do so. Indentation was carried out on longitudinal and transverse cross-sections of the UD CFRP material with the purpose of validating E1f, E2f, and Em. The subscripts "f" and "m" stand for fiber and matrix, respectively. The indentation was carried out using a CSM Instruments MCT tester (Needham, Massachusetts, United States of America). along order to get ten measurements, specimen cross-sections were wet sanded to a grit of FEPA P4000. These measurements were taken along a line with intervals of 10 µm. Due to the fact that the indentation modulus stabilizes at relatively high values [14,36,37], a depth of 0.1 µm was chosen for the indentation. On the other hand, deeper indentation was avoided in order to reduce the risk of fracture and maintain the continuity of the area function of the sphero-conical tip. After analyzing the data, it was clear which indentations had made contact with the fiber and which were located on the matrix. It was determined that the direction of the measurement line for the transverse sample was perpendicular to the direction of the fiber, which indicates that no two measurements were taken from the same filament. The settings for the indentation process are as follows: the indenter is a sphero-conical SB-B28, the tip radius is 2 µm, the cone full angle is 90°, the indentation depth is 0.1 µm, the loading rate is 0.8 mN/min, the dwell period is 30 seconds, and the data collection rate is 10 Hz.

Using the force-displacement data, the first unloading slope was calculated and established. Due to the fact that the power-law fit that is generally used and that was presented by Oliver and Pharr [38] did not generate high-correlation fits, a quadratic polynomial was taken into consideration. It was necessary to remove any permanent displacement (hf) from the data, and then it was necessary to impose intersection with the origin. For the purpose of determining the initial unloading slope, also known as contact stiffness, S [39], the derivative of the polynomial fit at maximum displacement was used. For the purpose of calculating the

contact depth (hc), the contact stiffness was used, and the value ε was set to 0.75, as suggested in reference [38]. Calculating the projected contact area and, thus, the indentation modulus M according to Vlassak's definition [40] required the use of the contact depth while doing so. When it is known what the parameters of the indenter are, it is simple to compute the indentation modulus of the isotropic matrix by utilizing the Oliver and Pharr technique [38]. In the case of an anisotropic material, where the contact area is circular, a different solution is used [41,42]. In this case, the concept is to solve all five stiffness constants by using a five-equation system. This is accomplished by including three previously known stiffness constants and two perpendicular indentation results via the system. The findings of a one-at-a-time sensitivity analysis revealed that none of the engineering constants that were added had a substantial impact on the outcomes on their own. For the purpose of the sensitivity analysis, each engineering constant was gradually increased or decreased by a factor of two or one-half. The values that were obtained for E2f were kept within a deviation of ten percent from the reference scenario. It was the indentation modulus that had the most significant impact, and its relationship was very close to being linear.

4. Results

When the simulation is finished, the results are given in the following order. To begin, the values that were measured are compared to the component qualities that were provided by the manufacturer. In addition, the micrographs that were used for meshing are given. Once the composite characteristics have been obtained, the second step is to generate the representative microstructure and then homogenize it. A comparison is made between the findings produced by analytical and experimental approaches on the other hand. Third, in order to generate loads that are relevant to the micromechanical model, macroscale simulations are brought into play. Lastly, carbon fiber reinforced plastic (CFRP) components are put through a failure test and compared to the simulated stresses and strains of the microstructures that correspond to them.

4.1. Constituent Properties

Within the micromodel, the component attributes and the microstructure are considered to be inputs. A list of material values for the constituents has been supplied by the manufacturer. As a result of the fact that this work only makes use of a single shear modulus, it is necessary to compute v23f by making use of the value of G23f that has been provided, taking into account the isotropic requirement.

For the purpose of verifying a few of the parameters that were provided, nanoindentation was carried out (Figure 4:1). The values that were supplied by the composite manufacturer are significantly different from the Young's moduli that were found from the indentation data (Table 2). [50] It has been claimed that nanobuckling and compressive failure in the nanostructure of carbon fiber are the reasons for the different behavior that might be seen in the case of the fiber. There have been other researchers that have got comparable outcomes for carbon fibers based on polyacrylonitrile [37,51,52,53]. The resultant E2f from these indentations is 13 GPa, which is in the middle of the 20 GPa that was provided by the manufacturer and the inverse micromechanics [14,17] that indicated that E2f should be 10

GPa during transverse compression testing. It is believed that the limitation that is imposed by the fibers that surround the epoxy is the cause of the different epoxy stiffness [53].

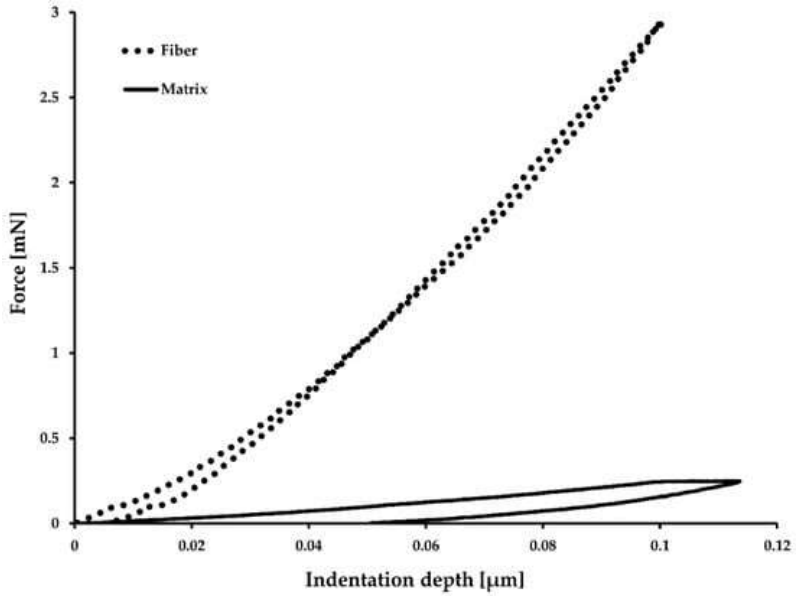

4.2 Effect of Defects

Utilizing the boundary conditions that were acquired from the macroscale hot spot analysis is the last stage in the multiscale modeling technique. This phase involves loading an RVE with a defect that is already discovered. A region of the microstructure that is abundant in resin is used to characterize the microstructure that has porosity. The absence of reinforcing fibers results in a localized increase in strain, and the fibers that are in close proximity to the area are required to bear the load. The flexural strength that was assessed, on the other hand, was not negatively impacted by this particular form of matrix fault. Porosity, on the other hand, leads to a reduction in the shear strength of the CFRP material, and failure occurs in the center plane (1-3) of the specimen, according to apparent ILSS testing. The influence of the resin-rich zone may be seen by modifying the RVE load scenario such that it corresponds with the failure site that was seen in the ILSS testing and then looking at the shear strain components. To be predicted, heterogeneities in the microstructure are responsible for local impacts, which may be evaluated by using the modeling technique that is provided in this article.

Industrial Engineering Journal
ISSN: 0970-2555
Volume : 50, Issue 9, No. 1, September : 2021

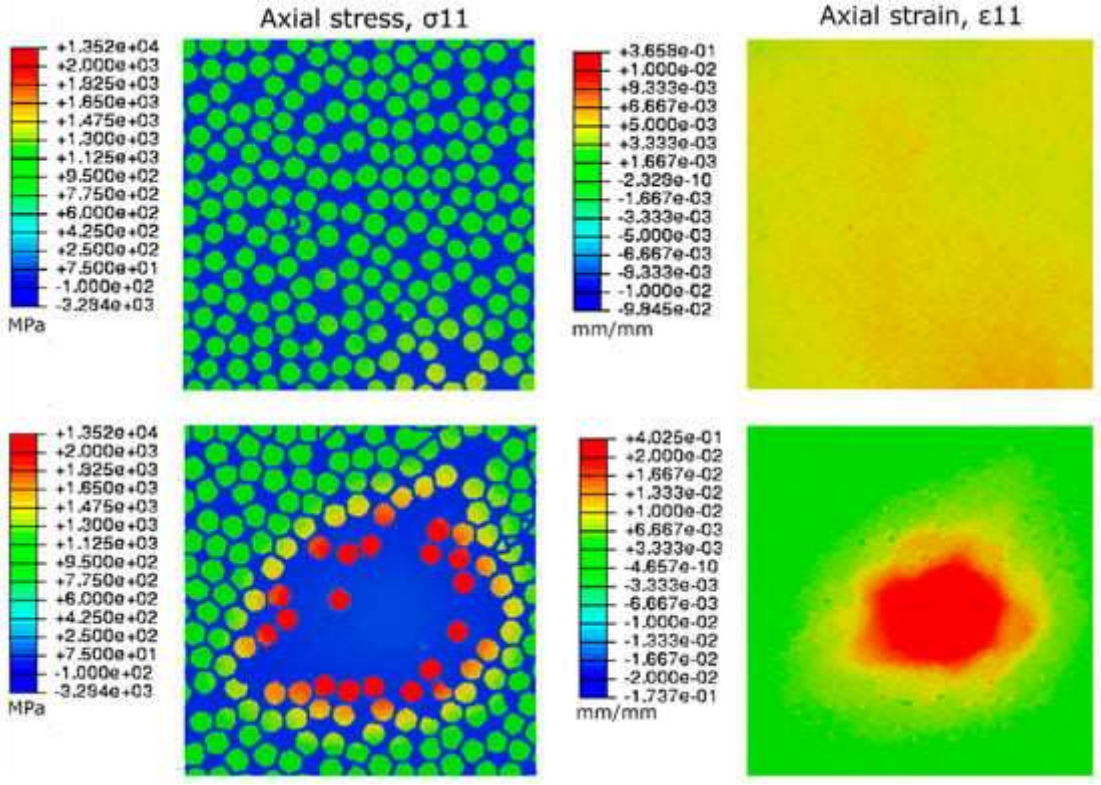

Figure 3. Comparison of reference microstructure (**top**) and resin-rich defect (**bottom**) in tension-dominated loading.

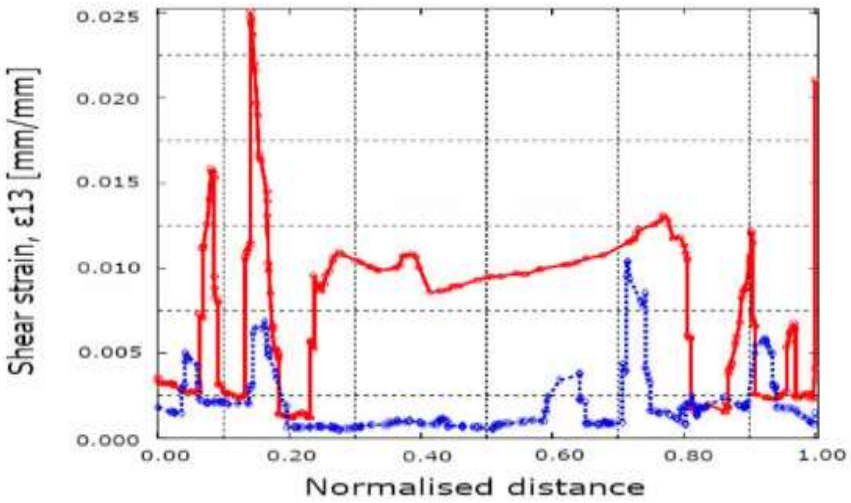

Figure 4. Line plots of the shear strains at the center (red) of the resin-rich microstructure and at the bottom (blue) in a shear-dominated load case.

5. Conclusion

To determine the impact that flaws have on unidirectional carbon fiber composites, a model that is based on micromechanics was developed. The following inputs are required for the

modeling approach: the characteristics of the fibers and resins, the microstructure, the macroscale load situations, the boundary conditions, and the design and position of defects. Due to the fact that the measuring technique is unknown, the fiber and resin qualities that are indicated by manufacturers should be accepted with care. Nanoindentation yields unsatisfactory results when it comes to determining the qualities of constituents, particularly with regard to the longitudinal fiber and matrix properties. Nanoscale bending of the fiber and a constraint effect in the matrix are two possible explanations for the phenomenon that has been seen there. The findings of the fiber's transverse nanoindentation were more comparable to the inverse micromechanics solutions and the literature values of fibers that were functionally equivalent. Homogenized composite characteristics were found to be in excellent agreement with experimental verifications, despite the fact that there was ambiguity in the input parameters. For the purpose of generating a mesh that is representational of the microstructure, SEM images were successfully segmented using an algorithm. The use of two-dimensional micrographs, on the other hand, does not take into account fiber waviness effects or defect morphology.

Both in terms of the elastic response and the site of failure, the results of the macroscale simulations were in excellent agreement with the actual data. It was determined via a sensitivity analysis that the only factor that has a substantial impact on the macroscale response is the longitudinal modulus of the composite of the material. In addition, the longitudinal fiber modulus, which is often not unknown, is the primary factor that influences that value. As a matter of fact, transverse characteristics are so negligible that an assumption of isotropic material properties only results in a three percent mistake in stress/strain relationships. Three-point bending, on the other hand, was the sole load instance that was used.

6. References

[1] Rizzo, P.; di Scalea, L. Acoustic emission monitoring of carbon-fiber-reinforced-polymer bridge stay cables in large-scale testing. Exp. Mech. 2001, 41, 282–290. [Google Scholar] [CrossRef]

[2] Rebel, G.; Verreet, R.; Ridge, I.M.L. Lightweight ropes for lifting applications. In Proceedings of the OIPEEC Conference, Athens, Greece, 27–29 March 2006; pp. 33–54. [Google Scholar]

[3] Antin, K.-N.; Machado, M.A.; Santos, T.G.; Vilaça, P. Evaluation of different non-destructive testing methods to detect imperfections in unidirectional carbon fiber composite ropes. J. Nondestruct. Eval. 2019, 38, 23. [Google Scholar] [CrossRef]

[4] Machado, M.A.; Antin, K.-N.; Rosado, L.S.; Vilaça, P.; Santos, T.G. Contactless high-speed eddy current inspection of unidirectional carbon fiber reinforced polymer. Compos. Part B Eng. 2019, 168, 226–235. [Google Scholar] [CrossRef]

[5] Hedgepeth, J.M.; van Dyke, P. Local stress concentrations in imperfect filamentary composite materials. J. Compos. Mater. 1967, 1, 294–309. [Google Scholar] [CrossRef]

[6] Landis, C.M.; McMeeking, R.M. Stress concentrations in composites with interface sliding, matrix stiffness and uneven fiber spacing using shear lag theory. Int. J. Solids Struct. 1999, 36, 4333–4361. [Google Scholar] [CrossRef]

[7] Otero, J.A.; Rodriguez-Ramos, R.; Bravo-Castillero, J.; Guinovart-Diaz, R.; Sabina, F.J.; Monsivais, G. Semi-analytical method for computing effective properties in elastic composite under imperfect contact. Int. J. Solids Struct. 2013, 50, 609–622. [Google Scholar] [CrossRef] [Green Version]

[8] Sun, C.T.; Vaidya, R.S. Prediction of composite properties from a representative volume element. Compos. Sci. Technol. 1996, 56, 171–179. [Google Scholar] [CrossRef]

[9] Mishnaevsky, L., Jr.; Broensted, P. Micromechanical modeling of damage and fracture of unidirectional fiber reinforced composites: A review. Comput. Mater. Sci. 2009, 44, 1351–1359. [Google Scholar] [CrossRef]

[10] Wongsto, A.; Li, S. Micromechanical FE analysis of UD fibre-reinforced composites with fibres distributed at random over the transverse cross-section. Compos. Part A 2005, 36, 1246–1266. [Google Scholar] [CrossRef]

[11] Dong, C. Effects of Process-Induced Voids on the Properties of Fibre Reinforced Composites. J. Mater. Sci. Technol. 2016, 7, 597–604. [Google Scholar] [CrossRef]

[12] Swolfs, Y.; Gorbatikh, L.; Romanov, V.S.; Orlova, S.; Lomov, S.V.; Verpoest, I. Stress concentrations in an impregnated fibre bundle with random fibre packing. Compos. Sci. Technol. 2013, 74, 113–120. [Google Scholar] [CrossRef]

[13] Vaughan, T.J.; McCarthy, C.T. Micromechanical modelling of the transverse damage behaviour in fibre reinforced composites. Compos. Sci. Technol. 2011, 71, 388–396. [Google Scholar] [CrossRef]

[14] Maurin, R.; Davies, P.; Baral, N.; Baley, C. Transverse properties of carbon fibres by nano-indentation and micro-mechanics. Appl. Compos. Mater. 2008, 15, 61–73. [Google Scholar] [CrossRef]

[15] Beicha, D.; Kanit, T.; Brunet, Y.; Imad, A.; El Moumen, A.; Khelfaoui, Y. Effective transverse elastic properties of unidirectional fiber reinforced composites. Mech. Mater. 2016, 102, 47–53. [Google Scholar] [CrossRef]

[16] Schumacher, D.; Antin, K.-N.; Zscherpel, U.; Vilaça, P. Application of different X-ray techniques to improve in-service carbon fiber reinforced rope inspection. J. Nondestruct. Eval. 2017, 36, 1–14. [Google Scholar] [CrossRef]

[17] Halpin, J.C.; Kardos, J.L. The Halpin-Tsai equations: A review. Polym. Eng. Sci. 1976, 16, 344–352. [Google Scholar]

[18] Sarlin, E.; von Essen, M.; Palola, S.; Lindgren, M.; Kallio, P.; Vuorinen, J. Determination of environmental degradation of matrix and fiber materials with a novel, stastically reliable micro-robotic approach. In Proceedings of the 17th European Conference on Composite Materials ECCM17, München, Germany, 26–30 June 2016. [Google Scholar]

[19] Ilankeeran, P.K.; Mohite, P.M.; Kamle, S. Axial tensile testing of single fibres. Mod. Mech. Eng. 2012, 2, 151–156. [Google Scholar] [CrossRef]

[20] Chamis, C.C. Simplified composite micromechanics equations for hygral, thermal and mechanical properties. NASA Technical Memorandum 83320. In Proceedings of the 38th Annual Conference of the Society of the Plastics Industry, Houston, TX, USA, 7–11 February 1983. [Google Scholar]

[21] Mounier, D.; Poilane, C.; Bucher, C.; Picart, P. Evaluation of transverse elastic properties of fibers used in composite materials by laser resonant ultrasound spectroscopy. In Proceedings of the Acoustics Conference, Nantes, France, 23–27 April 2012. [Google Scholar]

[22] Soden, P.D.; Hinton, M.J.; Kaddour, A.S. Lamina properties, lay-up configurations and loading conditions for a range of fibre-reinforced composite laminates. Compos. Sci. Technol. 1998, 58, 1011–1022. [Google Scholar] [CrossRef]

[23] Turon, A.; Costa, J.; Maimi, P.; Trias, D.; Mayugo, J.A. A progressive damage model for unidirectional fibre-reinforced composites based on fibre fragmentation. Part I: Formulation. Compos. Sci. Technol. 2005, 65, 2039–2048. [Google Scholar] [CrossRef]

[24] Blassiau, S.; Thionnet, A.; Bunsell, A.R. Micromechanisms of load transfer in a unidirectional carbon fibre–reinforced epoxy composite due to fibre failures. Part 1: Micromechanisms and 3D analysis of load transfer: The elastic case. Compos. Struct. 2006, 74, 303–318. [Google Scholar] [CrossRef]

[25] Behzadi, S.; Jones, F.R. The effect of temperature on stress transfer between a broken fibre and the adjacent fibres in unidirectional fibre composites. Compos. Sci. Technol. 2010, 68, 2690–2696. [Google Scholar] [CrossRef]

[26] Bouaoune, L.; Brunet, Y.; El Moumen, A.; Kanit, T.; Mazouz, H. Random versus periodic microstructures for elasticity of fibers reinforced composites. Compos. Part B 2016, 103, 68–73. [Google Scholar] [CrossRef]

[27] Melro, A.R.; Camanho, P.P.; Pinho, S.T. Generation of random distribution of fibres in long-fibre reinforced composites. Compos. Sci. Technol. 2008, 68, 2092–2102. [Google Scholar] [CrossRef]

[28] Swolfs, Y.; Verpoest, I.; Gorbatikh, L. Issues in strength models for unidirectional fibre-reinforced composites related to Weibull distributions, fibre packings and boundary effects. Compos. Sci. Technol. 2015, 114, 42–49. [Google Scholar] [CrossRef] [Green Version]

[29] Okabe, T.; Takeda, N.; Kamoshida, Y.; Shimizu, M.; Curtin, W.A. A 3D shear-lag model considering micro-damage and statistical strength prediction of unidirectional fiber-reinforced composites. Compos. Sci. Technol. 2001, 61, 1773–1787. [Google Scholar] [CrossRef]

[30] Trias, D.; Costa, J.; Mayugo, J.A.; Hurtado, J.E. Random models versus periodic models for fibre reinforced composites. Comput. Mater. Sci. 2006, 38, 316–324. [Google Scholar] [CrossRef]

[31] Holmberg, K.; Laukkanen, A.; Turunen, E.; Laitinen, T. Wear resistance optimisation of composite coatings by computational microstructural modelling. Surf. Coat. Technol. 2014, 247, 1–13. [Google Scholar] [CrossRef]

[32] Orell, O.; Vuorinen, J.; Jokinen, J.; Kettunen, H.; Hytönen, P.; Turunen, J.; Kanerva, M. Characterization of elastic constants of anisotropic composites in compression using digital image correlation. Compos. Struct. 2018, 185, 176–185. [Google Scholar] [CrossRef]

[33] Haj-Ali, R.; Kilic, H. Nonlinear constitutive model for pultruded FRP composites. Mech. Mater. 2003, 35, 791–801. [Google Scholar] [CrossRef]

[34] Fiedler, B.; Holst, S.; Hobbiebrunken, T.; Hojo, M.; Schulte, K. Modelling of the initial failure of CFRP structures by partial discretisation: A micro/macro-mechanical approach of first ply failure. Adv. Compos. Lett. 2004, 13. [Google Scholar] [CrossRef]

[35] Fliegener, S.; Luke, M.; Gumbsch, P. 3D microstructure modeling of long fiber reinforced thermoplastics. Compos. Sci. Technol. 2014, 104, 136–145. [Google Scholar] [CrossRef]

[36] Miyagawa, H.; Mase, T.; Sato, C.; Drown, E.; Drzal, L.T.; Ikegami, K. Comparison of experimental and theoretical transverse elastic modulus of carbon fibers. Carbon 2006, 44, 2002–2008. [Google Scholar] [CrossRef]